An Ionic Liquid Reaction and Separation Process for Production of Hydroxymethylfurfural from Sugars

Wei Liu, Feng (Richard) Zheng, Joanne Li, and Alan Cooper
Energy and Environment Directorate, Pacific Northwest National Laboratory, Richland, WA 99352

DOI 10.1002/aic.14289
Published online November 22, 2013 in Wiley Online Library (wileyonlinelibrary.com)

Hydroxymethylfurfural (HMF) is viewed as a potential platform material to make a variety of chemicals and products out of renewable resources. In this work, a complete ionic liquid reaction and separation process is presented for nearly stoichiometric conversion of fructose into HMF. The silicalite adsorbent material is demonstrated for separation of 99% pure HMF out of ionic liquid reaction mixtures through a packed column and for recovery of the unconverted sugars and reaction intermediates along with the ionic liquid. Membrane-coated silicalite particles are prepared and studied for a practical adsorption process with separation performances comparable to or better than the powder material. It is discovered that nearly all the fresh fructose feed could be converted into HMF with the recycled ionic liquid under suitable reaction conditions. These research results lead to a new HMF production process much simpler than the current paraxylene manufacturing process from petroleum oil. © 2013 American Institute of Chemical Engineers *AIChE J*, 60: 300–314, 2014

Keywords: ionic liquid, hydroxymethylfurfural, plastics, sugar, biomass, adsorption, reaction, separation, membrane, adsorbent

Introduction

Manufacturing of polymeric products out of renewable biomass feedstock instead of petroleum oil has received a great interest for recent years.[1–4] Hydroxymethylfurfural (HMF) has been viewed as a potential platform material to make a variety of chemicals and products.[5,6] For example, HMF can be converted into 2,5-furan dicarboxylic acid via selective oxidation as an alternative to petroleum-derived paraxylene (PX)-terephthalic acid product chain[7] for polyester production. Information in various aspects of HMF from conversion chemistry, process development, to applications can be found in recent reviews.[8,9] In addition to chemical values, diesel-range biofuels may be produced from HMF or furfural through esterification and condensation reactions.[10]

Production of HMF at a cost competitive with existing products is the key to realizing all the exciting application opportunities. Stoichiometrically, HMF is a sugar molecule minus three water molecules. Sugars can be produced in large quantities by agriculture or prepared from degradation and decomposition of nonfood grade biomass raw materials. Dehydration of sugars into HMF is attractive from points of view of both carbon number efficiency and sustainability. A great amount of studies have been published around catalytic conversion of sugars into HMF. A snapshot of various catalytic approaches can be found in the reviews.[8,9,11] Aqueous-organic biphasic reaction systems were studied for simultaneous extraction of HMF product during catalytic dehydration of fructose.[12–14] The reaction is conducted at about 180°C in presence of a HCl catalyst, requiring high-pressure, corrosion-resistant reactors. Besides, there is significant formation of byproducts. As a result, high production cost was projected relative to current PX product.[13,14]

The ionic liquid (IL) as a solvent medium can be used at elevated temperatures (100–200°C) under atmospheric pressures, because of its nonvolatility. Thus, it has received substantial interest for development of new separation and reaction processes for recent years. It was discovered that conversion of sugars (fructose and glucose) into HMF can be conducted in the IL under moderate conditions with both high activity and selectivity.[15] Furthermore, HMF and derivatives can be produced via selective breakdown of cellulose and lignocelluloses in an IL catalyst system.[16,17] Broad applications of the IL to biomass pretreatment and conversion were reviewed in recent publications.[18,19] However, a complete process loop related to IL catalytic reaction and separation has not been closed yet. Compared to extensive catalysis chemistry studies, original research reports on separation of reaction mixtures and delineation of reaction byproducts have been scarce.

In this work, we try to tackle some fundamental problems for development of an economic HMF production process from sugars, such as separation of pure HMF from reaction mixtures, demonstration of reusability of the IL, and identification and disposal of reaction byproducts. The IL used in this work was discovered from our previous catalysis

This article was nominated by Professor Suojiang Zhang (Institute of Process Engineering, Chinese Academy of Sciences) – section chair of International Forum on Energy Sustainability as the Best Presentation during the AIChE Annual Meeting in Pittsburgh, PA, Oct. 28-Nov. 2, 2012.

Correspondence concerning this article should be addressed to W. Liu at wei.liu@pnnl.gov.

Table 1. Surface Areas and Pore Volumes of Adsorbent Materials

Sample Name	Multipoint BET Surface Area (m^2/g)	t-Method Micropore Surface Area (m^2/g)	t-Method Micropore Volume (cm^3/g)	BJH Method Mesopore Volume (cm^3/g)
Organic-philic zeolite (OPZ) powder	337	89.7	0.04	0.18
Silicalite-coated OPZ particle	406	128	0.05	0.18
Nano-silicalite powder	416	255	0.10	0.13
Silicalite-coated silicalite particle	398	295	0.11	0.09

research studies,[20] which is relatively inexpensive and can be available in large quantities. Different from previous solvent extraction and polymeric resin adsorbents,[21] a zeolite adsorption process is chosen based on an earlier invention made by this research group.[22] Out of a variety of adsorbent materials screened, silicalite was identified as the most effective for selective adsorption of HMF from various IL and/or water mixtures. Its molecular specificity is attributed to the size exclusion function of this type of zeolite lattice framework and unique surface chemistry. Silicalite-type materials also have excellent thermal and chemical stability so that the adsorbent can be used over a wide range of adsorption and desorption conditions. The other consideration is that there are several successful examples for zeolite adsorption separation in current refining and petrochemical separation processes, such as separation of PX from C8 aromatics. Fructose is used as the feedstock for the present process research activities.

Experimental Section

Materials

Triisobutylmethylphosphonium tosylate (Cyphos 106, 99% purity, Cytec) was used in most experiments in this work, whereas 1-ethyl-3-methyl imidazolium chloride −[EMIM]Cl (94% purity, BASF) was tested for cellulose reactions. Both ILs were used as received. Unless specifically noted, the IL used in the experiments refers to Cyphos 106. Fructose (99.5%, Sigma-Aldrich), deionized water, and methanol (99.5%, Sigma-Aldrich) were used as the sugar feed, dilution fluid, and flushing solvent for HMF desorption, respectively. 5-Hydroxymethylfurfural (98.5%, Sigma-Aldrich) was used as a reference.

Table 1 lists the adsorbent powder and particle materials studied in this work. Organophilic zeolite (OPZ) powder was acquired from Aldrich. Silicalite powder was prepared in-house with the detailed preparation procedure reported in our earlier publication.[23] Engineered adsorbent particles were prepared by deposition of a silicalite membrane on the exterior surface of the powder material that was pelletized, crushed, and sieved into 40–140 mesh. The membrane deposition is similar to the secondary growth method used for preparation of a flat sheet zeolite membrane.[24] All the adsorbent materials were calcined at 550°C for 5 h with the ramping rate of 1°C/min prior to adsorption tests.

Characterization of adsorbents, IL, and HMF product

Surface area, porosity, and pore-size measurements of the adsorbent material were conducted by nitrogen adsorption/desorption on a Quantachrome Autosorb 6-B gas sorption system. All the samples were degassed at 300°C prior to the measurement. The surface area was determined using Brunauer–Emmett–Teller (BET) method. Barrett–Joyner–Halenda method was used for analysis of the porosity and pore size, whereas T method was used for micropore analysis. Scanning Electron Microscopy (SEM) analysis was performed on JEOL JSM-5900, and the cross-section of the adsorbent particle was prepared using a procedure as described for the zeolite/metal sheet membrane samples previously.[24] The X-ray diffraction (XRD) of adsorbent materials was measured at a scan rate of 0.04°/min using a Bruker D8 Advance diffractometer with 0.154098 nm Cu Kα radiation and a graphite monochromator. The viscosity of ILs was measured using an Anton Paar Stabinger Viscometer (SVM3000).

HMF product isolated in this work was characterized by Thermogravimetric Analyzer (TGA) integrated with differential scanning calorimetry (DSC) measurements. The measurement was conducted on QMS 403 C Aeolos-Quadrupole Mass Spectrometer from Netzsch. Argon gas was used as a carrier and purge gas. About 10 mg of HMF placed in the sample pan was heated in a dry inert gas stream (Ar) from room temperature to 200°C at 2°C/min.

Batch reactor tests

The reaction test was conducted in a batch glass reactor under continuous stirring. The free space of the reactor was purged by a continuous N_2 gas flow under atmospheric pressure. The detailed procedure and results for reaction of sugar in various ILs were described in the previous publication by this research team.[20] For assessment of reactivity of the recycled IL, the IL was placed into the reactor, gradually heated up, and sampled at different temperatures for analysis. For reaction kinetics measurements of fresh fructose in the recycled IL, the IL was sampled for analysis when the reactor temperature was stabilized at a target level; fructose feed was added into the IL; the reacting mixture was sampled for analysis at different times at a constant temperature.

Adsorption column tests

Packing of the adsorption bed with powder materials was conducted by pumping powder/methanol slurry into a standard chromatograph column under a constant pressure. The pump was stopped when the pressure started rising rapidly. Methanol was dried prior to use. Packing of engineered particles was conducted by simply pouring dry particles into a metal tube with a nickel metal foam disk plugged at the bottom while the tube wall was slightly tapped. The void space in the column was determined based on the methanol uptake measured from the weight difference of the column between the wet and dried state. The wet state represents the adsorbent bed fully soaked with methanol liquid at room

Table 2. HPLC Elution Times of Individual Components in an Ionic Reaction Mixture

Peak Name	Retention Time (min)	Response Factor Area/%	Symbol	Constituent
Ionic liquid	6.9	278,714	IL	Major
Unknown	7.7	NA	Unk	Some
Unknown	8.4	NA		
Unknown	8.8	NA		
Glucose	9.4	497,929	Glu	Minor
Fructose	10.4	490,993	Fru	Some
Unknown	10.9	NA	Unk	Insignificant
Unknown	12.1	NA		
Formic acid	15.2	149,787	FA	Trace
Levulinic acid	18.2	361,915	LA	None
Hydroxymethylfurfural	38.4	587,977	HMF	Significant

temperature, whereas the bed is regarded in the dried state after the wet bed was dried at 70°C overnight.

The packed column was tested for adsorption under a consistent temperature (typically 50°C) and feed flow rate. The feed mixture was prepared by quenching the fructose IL reaction mixture with deionized water at about 1:1 weight ratio. The raffinate existing from the column was periodically collected and analyzed to obtain the adsorption breakthrough curve. Unless specifically noted, a standard procedure used for regeneration of the saturated column consisted of (1) purging the column and line by nitrogen gas for removal of the bulk feed solution retained in the system, (2) washing the column by deionized water for removal of residual IL, and (3) washing the column by methanol for desorption of adsorbed HMF. During regeneration, the column effluent was periodically collected and analyzed to obtain regeneration profiles.

The effluent collected during the methanol flushing, which was substantially free of IL, was used for isolation of pure HMF product. The raffinate and water-flushing effluents were collected and combined for recovery of ILs. Methanol and water were removed from the collected liquid sample by using Rotatory Evaporation under 10 torr and High Vacuum Schlenk Line under 83 mtorr. The glass flask used for evaporation was wrapped with Al foil to block light irradiation. All the evaporative drying processes were conducted at room temperature to minimize side reactions.

Compositional analysis of liquid samples

Liquid-phase samples were obtained from the reaction and adsorption tests. The as-produced sample was diluted with an appropriate amount of deionized water to a level within the linear response range of high-performance liquid chromatography (HPLC) analysis. Agilent 1100 series HPLC equipped with Agilent G1362A refractive index Detector was used. The analytical column used was BioRad Aminex HPX-87H (300 × 7.8 mm^2). The column temperature was maintained at 60°C and a 0.005 M H_2SO_4 solution was used as the mobile phase at a flow rate of 0.9 cm^3/min. In the HPLC analysis, individual compounds are distinguished based on their retention times by comparing to the calibration standards. Table 2 lists the retention times of peaks detected in typical HPLC analyses of reacted IL mixtures. It is noted that several peaks with retention times between the IL and glucose were clearly detected by HPLC but could not be identified with known compounds presently. The reaction products with retention times between the fructose and formic acid were insignificant in terms of peak area relative to HMF. In this work, the peaks of all those unknown products are lumped together and denoted as "Unk." Its content is estimated by assuming a response factor same as fructose.

Unless specifically noted, all the percentage (%) reported in this article is weight based

Results and Discussions

Viscosity of IL

High viscosity and slow mass transport were considered the main problems for IL separation processes. In Figure 1a, viscosity of the IL used in this work is compared with water and light mineral oil at various temperatures. At a low temperature (40°C), viscosity of the pure IL[25] is about 1 and 2 orders of magnitude higher than the respective water[26] and mineral oil. However, the IL viscosity decreases exponentially with increasing temperature. At 110°C, the viscosity becomes close to that of the mineral oil at 40°C. As the IL is stable and not volatile up to 200°C, the viscosity issue can be mitigated by conducting the catalytic or separation processes at elevated temperatures. Another way to reduce the viscosity is to mix the IL with water. Figure 1b shows that

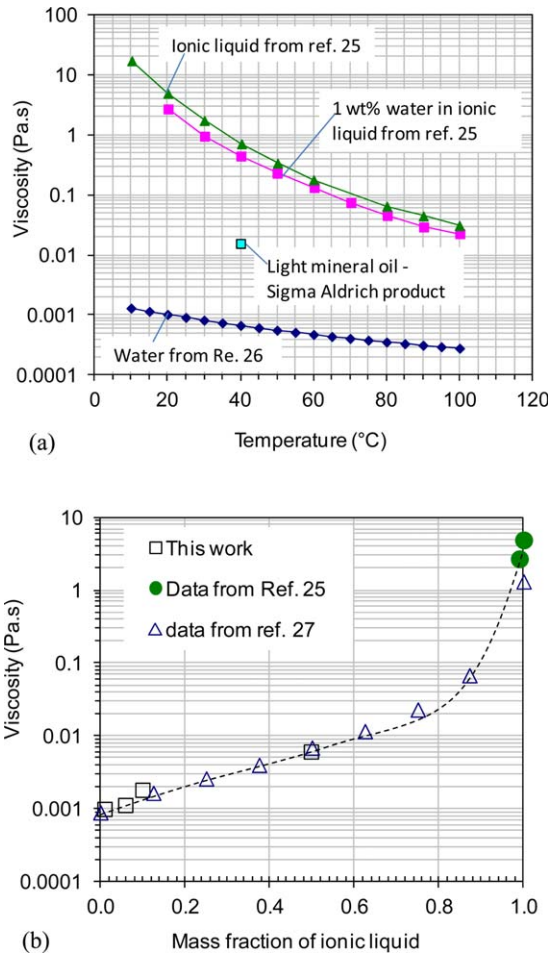

Figure 1. Viscosity of triisobutylmethylphosphonium tosylate IL used in this work

(a) Variation of viscosity with temperature and (b) variation of viscosity with IL content in water IL mixture ($T = 20$°C). [Color figure can be viewed in the online issue, which is available at wileyonlinelibrary.com.]

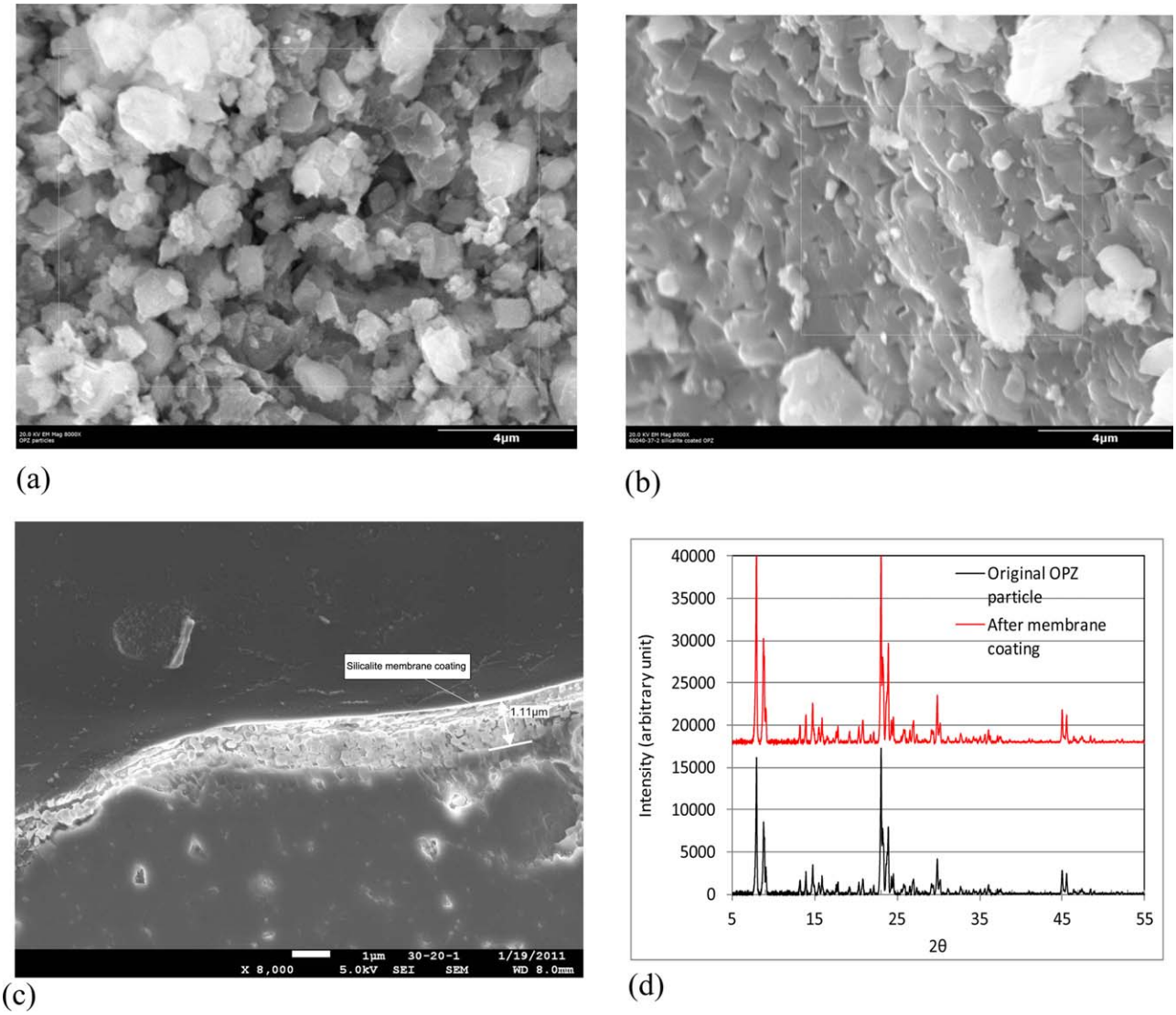

Figure 2. Structures of OPZ particles before and after silicalite membrane coating.

(a) Surface of OPZ particle before coating, (b) surface texture after membrane coating, (c) cross-section of membrane-coated particle, and (d) XRD patterns. [Color figure can be viewed in the online issue, which is available at wileyonlinelibrary.com.]

the viscosity of the IL/water mixture exponentially decreases with increasing water loading in the mixture. The viscosity values measured in this work are in line with the literature data.[25,27] The viscosity of a 50% IL in water mixture at 20°C is even lower than the mineral oil at 40°C. Thus, concerns about high viscosity of the IL for practical processes can be addressed by increasing the process temperature and/or adding water.

Characterization results of adsorbent materials

The surface areas and pore volumes of adsorbent materials evaluated in this work are summarized in Table 1. The BET surface area is contributed by both micro and mesopores. The former is considered as well-defined channels in the zeolite framework, whereas the latter can be attributed to exterior surfaces and defects of zeolite crystals. The OPZ powder has a small micropore volume and a small fraction of micropore surface area, compared to the nano-silicalite materials prepared in this work. It is worth noting that the original zeolite micropores were not plugged by the zeolite membrane coating. Instead, the micropore surface area was increased from 89.7 for the original powder to128 m^2/g for the OPZ particle. A significant increase in the micropore surface area was also observed with the nano-silicalite particle. The increase can be explained by conversion of some amorphous material in the original powder into zeolite crystals during the membrane growth.

The microstructures of the engineered particle before and after membrane coating were analyzed by SEM. The microstructural characteristic is compared in Figures 2 and 3 for the OPZ and nano-silicalite particle, respectively. The as-pelletized OPZ particle has a rough surface texture comprised of large and irregular agglomerates (of crystals) and voids (Figure 2a). The particle surface became dense and uniform after the membrane coating (Figure 2b). The coating layer comprises intergrown zeolite crystals. The cross-sectional analysis (Figure 2c) reveals the membrane thickness on this particle is about 1.1 μm. Figure 2d shows identical XRD patterns for the OPZ adsorbent before and after

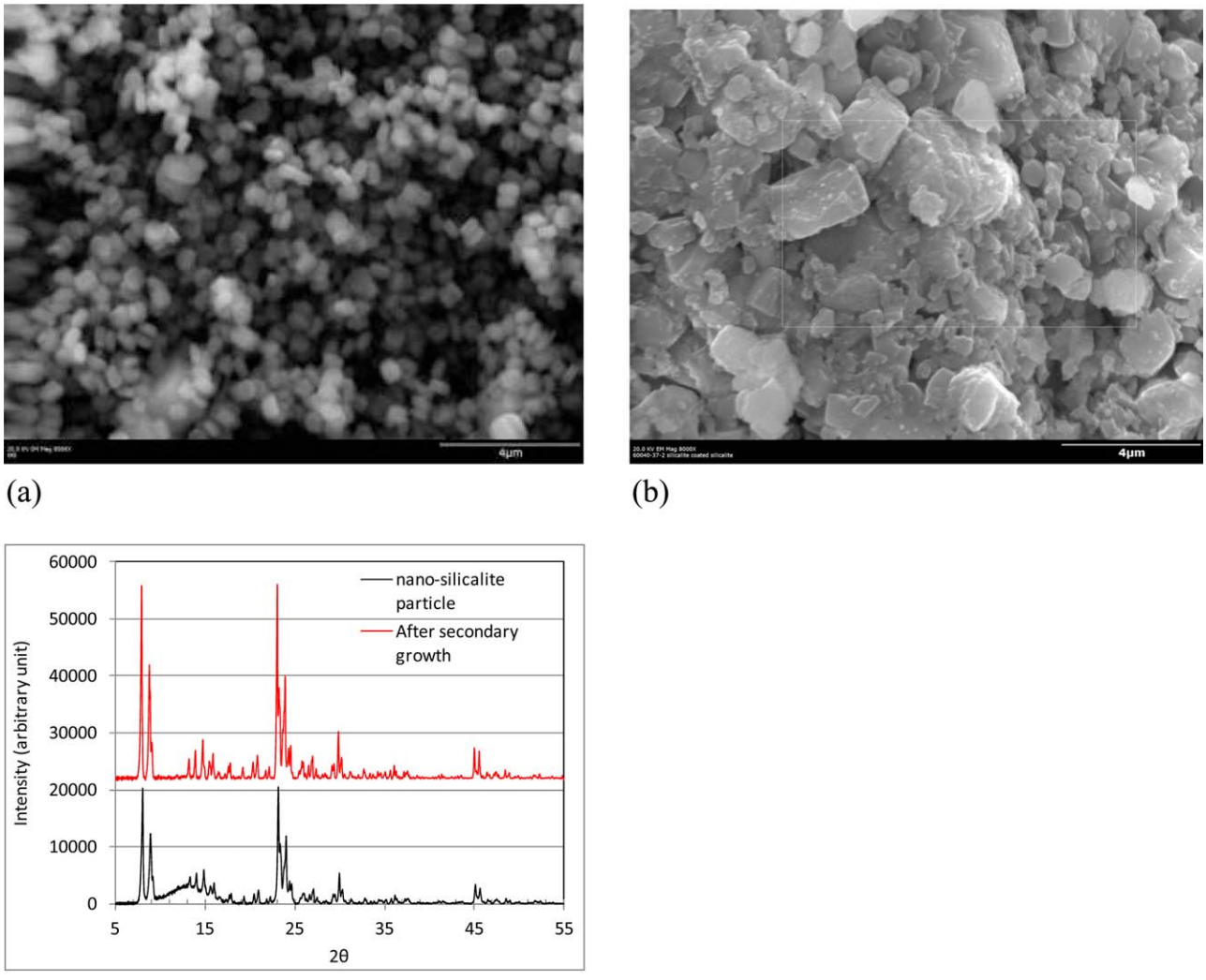

Figure 3. Structures of a silicalite particle before and after membrane growth

(a) Surface of a pelletized particle, (b) surface of regrown particle, and (c) XRD patterns. [Color figure can be viewed in the online issue, which is available at wileyonlinelibrary.com.]

membrane coating, which confirm the same MFI-type zeolite crystal phase. The peak intensity after membrane growth appears higher than the parent particle, indicating enhanced zeolite crystal growth during membrane preparation. The XRD observation is consistent with the increased micropore surface area.

Figure 3a shows that the nano-silicalite powder comprises uniform, individual crystals without intercrystal bonding. In the experiments, we found that the particle made from pelletization of this powder material was very weak and easily collapsed into loose powder with slight crushing. After the membrane growth, the loose crystals were bonded together through intercrystal growth and the resulting particles were fairly strong. As shown in Figure 3b, the surface texture of the membrane-coated particle is indeed much denser than the pelletized powder. The XRD patterns (Figure 2c) before and after the membrane coating look same. The much higher peak intensity of the regrown particle confirms zeolite crystal growth enhanced under the membrane growth conditions. The enhanced growth of parent crystals results in an increase in the micropore surface area (Table 1) and strengthens the particle.

Separation of reacted mixtures on columns packed with adsorbent powder

A significant amount of effort was devoted toward optimizing column packing and operation conditions to obtain 99% pure HMF product from IL reaction mixtures.[20] The same OPZ powder was packed into two different sizes of columns. A uniform feed flow could not be obtained with the column of 22 mm ID and 70 mm length, because the adsorption and regeneration profiles were associated with serious tailing and channeling. The aspect ratio (length/diameter = 3.2) of that column was determined too small to establish a plug flow. Thus, all the adsorption separation tests latter were conducted using 10 mm ID × 250 mm length column (aspect ratio = 25). The adsorbent packing density and bed void fraction with this size of column is listed in Table 3.

With the column of a high aspect ratio, both OPZ and nano-silicalite powder provided excellent performances for separation of HMF out of reacted IL mixtures. However, the nano-silicalite powder presented large pressure drops, which was mostly due to its high packing density and small crystal size. The large pressure drop limited adsorption/regeneration

Table 3. Adsorption Bed Loading (Column size: 10 mm ID × 250 mm length for powder and 7 mm ID × 250 mm length for particles)

Column Name	Adsorbent Material	Loading (g)	Packing Density (g/cm^3)	Void Fraction
OPZ powder	As-received OPZ powder	14.6	0.74	0.61
Nano-silicalite powder	Nano-silicalite powder synthesized in-house	19.0	0.97	0.51
Silicalite/OPZ particle	45–140 mesh of silicalite-coated OPZ particles	11.5	9.5	0.49
Silicalite/silicalite particle	45–140 mesh of silicalite-coated silicalite particles	10.6	6.9	0.35

tests to a narrow range of flow rates. As a result, the OPZ powder column was chosen for extensive adsorption and regeneration process studies. This column allowed tests being conducted over a range of feed flow rate (0.5–2.5 cm^3/min) and desorption flow rate (0.5–10 cm^3/min).

One major challenge to obtaining pure HMF is complete washing of residual IL out of the adsorbent bed prior to HMF desorption. Different flow rates and times, and different washing fluids were tried to purge the IL out of the column after the adsorption was done. Finally, an effective regeneration protocol was identified that enabled isolation of pure HMF from the desorption effluent. The representative adsorption breakthrough and desorption profiles are shown in Figures 4a and b, respectively. The feed used for this adsorption run was prepared by reacting fructose in the fresh IL at 110°C and consisted of 48.6% IL, 0.45% fructose (Fru), 1.23% unknown (Unk), 2.48% HMF, and balance water. As glucose, formic acid, and levulinic acid did not exist in the feed solution, they are not shown in the plots. During adsorption run (Figure 4a), the IL, fructose (Fru), and unknown (Unk) came out together as the feed passed through the column. It took about 90 min for HMF breakthrough to occur. During regeneration (Figure 4b), the IL and fructose (Fru) retained among interparticle voids were rapidly washed out by water, whereas the adsorbed HMF inside the zeolite pore was intact. Upon switching to methanol flushing, HMF came out gradually, reached a peak, and then, declined to zero. Compared to 2.48% loading in the adsorption feed, HMF content in the methanol effluent was as high as 34% at the peak. Dramatic enrichment of HMF was realized by the present adsorption separation. A majority of the unknown products (Unk) was washed out of the column by water, but some unknown species emerged in the late stage of the methanol flushing in this particular run.

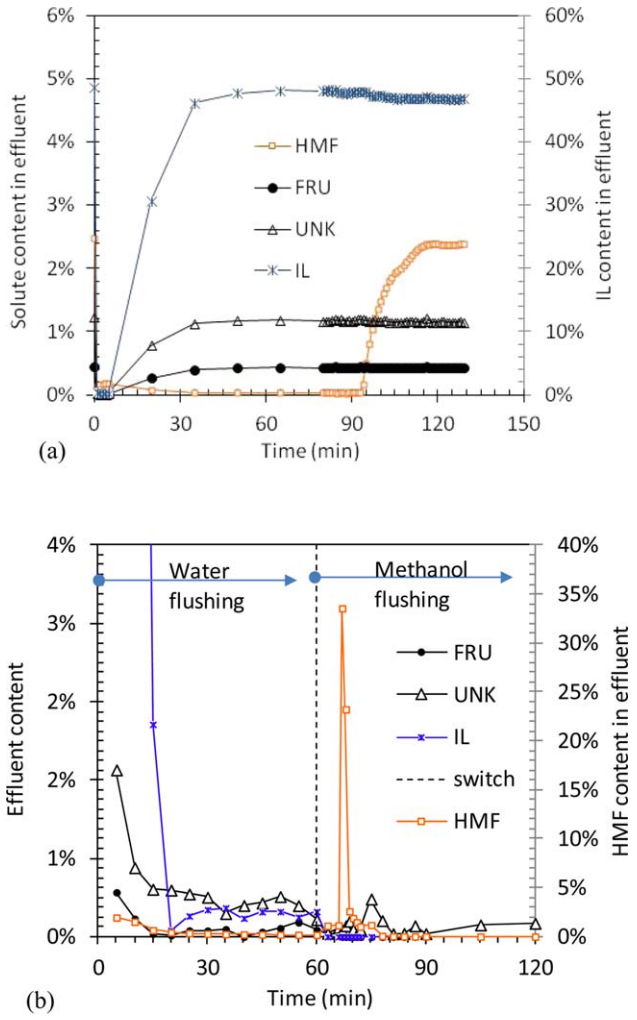

Figure 4. Adsorption and regeneration profiles of OPZ powder-packed column (adsorption feed composition: 48.6% IL, 2.48% HMF, 0.45% Fru, 1.23% Unk, and balance water)

(a) Adsorption breakthrough profiles (50°C, feed rate of 0.945 cm^3/min) and (b) regeneration profiles (50°C, feed rate of 2.06 cm^3/min). [Color figure can be viewed in the online issue, which is available at wileyonlinelibrary.com.]

The OPZ powder column was tested with multiple adsorption/regeneration cycles with various IL reaction mixtures. The working capacity as determined based on the amount of HMF collected in desorption effluent was stabilized around 12.0%.

Isolation of pure HMF and recovery of IL from reacted IL mixture

Based on the regeneration profiles (Figure 4b), the first two methanol-flushing effluents (peak and next to the peak) were collected for isolation of pure HMF. Figure 5 shows appearance of the recovered IL and isolated HMF product after water and methanol solvents were substantially removed. The pure IL has a melting point of 42°C. The recovered IL stayed in liquid phase at room temperature because small amounts of water remained after the vacuum drying. Purity of the HMF isolated from four adsorption/regeneration cycles is listed in Table 4. These runs were performed on different days, and there was slight variation in the adsorption feed composition. >98% pure HMF was consistently obtained from the methanol effluent at the peak position. The purity of the HMF concentrated from another methanol effluent varied due to presence of residual IL and some unknown species.

For the adsorption cycle #5 in Table 4, 98.1% of the IL fed through the column was recovered from the raffinate and

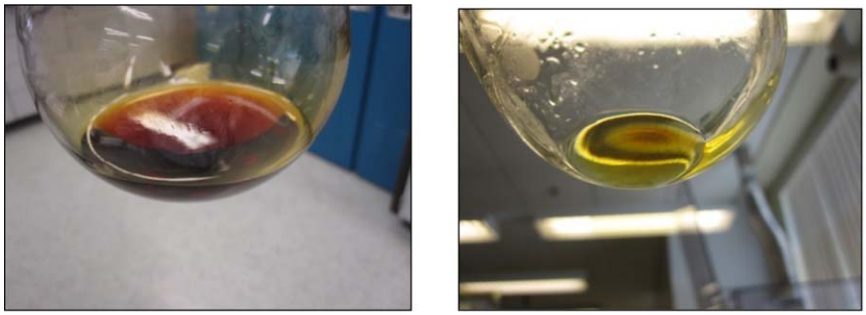

(a) (b)

Figure 5. Appearance of recovered IL and HMF from adsorption separation process (OPZ column)

(a) 95.0% IL from raffinate and (b) 98.5% HMF from methanol extract. [Color figure can be viewed in the online issue, which is available at wileyonlinelibrary.com.]

water-flushing effluent. For HMF, the mass balance (out/in) was only 94.2%. The IL recovery and HMF mass balance did not change much in the other adsorption cycles. Stability of HMF during the experimental process was concerned initially. To check stability of HMF under the adsorption and desorption conditions, we ran a complete adsorption/regeneration cycle with a model feed containing 2% HMF in water. No new peaks were found in the HPLC analyses of column effluents, which confirmed that HMF was stable under the present adsorption/regeneration conditions. To check the stability of HMF during the product concentration process, we dissolved 2% HMF in methanol and ran it through the Rotovap and Schlenk line vacuum drying process. The resulting HMF had the same composition as its starting material, and no other new species were detected by the HPLC analysis. Stability of HMF under storage was examined through comparative experiments. The results indicate that HMF could be very reactive in ambient air conditions and under light irradiation, which is likely due to air oxidation and polymerization reactions. Thus, less than 100% recovery of the IL was mostly due to incidental loss during the experiment, whereas low HMF recovery was attributed to both the incidental loss and degradation of HMF samples during storage under ambient conditions.

The HMF product isolated above was characterized on TGA/DSC. A HMF sample purchased from Aldrich was tested under the same conditions for comparison. A large thermal flux peak was observed at 35°C for both samples, which indicates the same phase change point of HMF from crystalline into liquid. The gradual weight loss started around 100°C for the two samples. The weight loss rate accelerated with increasing temperature. The heat of HMF vaporization was calculated from the Arrhenius plots of evaporation rate versus T over a temperature range of 100 and 180°C. The resulting heat of vaporization values are 68.5 and 69.0 kJ/mol for the reference and recovered HMF, respectively, which are very close.

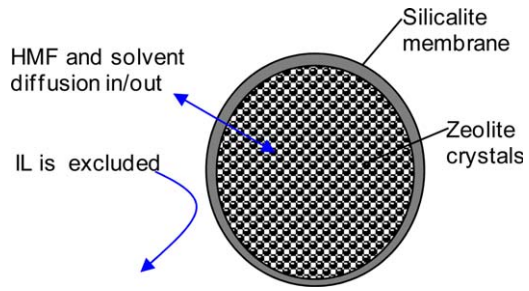

Figure 6. Working principle of membrane-coated adsorbent particle.

[Color figure can be viewed in the online issue, which is available at wileyonlinelibrary.com.]

Membrane-coated adsorbent particles for a practical adsorption process

The feasibility to isolate pure HMF product with the adsorbent powder material was successfully shown above. However, the pressure drop of powder-packed columns is too large to be practical. The difficulty to obtain complete purge of the residual IL out of the powder-packed column by water is another concern. Thus, preparation of engineered particles was studied. One problem to make engineered particles out of the silicalite powder is lack of bonding between pure silicalite crystals. Using binders such as colloidal alumina and silica solutions can alter the adsorbent properties. It is known that Al atoms can incorporate into silicalite framework to form ZSM-5 during the hydrothermal preparation. ZSM-5 is more hydrophilic than pure silicalite. Hydrophobicity of the silicalite material is preferred for the present adsorption process, which allows exclusion of water from the zeolite pores and ready uptake of organic solvent into the pore for HMF desorption. The silica binders are typically hydrophilic as well. Another main problem is retention of the IL inside pores of an engineered particle. The conventional adsorbent particle often contains irregular macropores. The IL trapped in those pores during adsorption can become very difficult to be purged out due to its low diffusivity.

To address these problems, we engineered the adsorbent particle in a different way from conventional approaches. As illustrated in Figure 6, a particle comprised of zeolite crystals is encapsulated with a thin (<10 μm) silicalite membrane layer. In this way, penetration of ILs into the interior of the particle is blocked by the membrane, whereas the micropores of the silicalite membrane allow for HMF and solvent molecules to transport between the interior of the particle and bulk fluid. The silicalite membrane layer is so thin relative to the particle size that it does not impose significant mass-transfer resistance.

Table 3 lists the two columns packed with the silicalite/OPZ and silicalite/silicalite particles, respectively. The adsorption breakthrough profiles for the silicalite/OPZ particle (Figure 7a) show simultaneous elution of fructose and unknown (Unk) with the IL upon introduction of the feed and nearly constant pressure drop of 0.96 bars across the

Table 4. Purity of HMF Produced by Adsorption Separation (OPZ Powder Column)

	Water-Quenched Reaction Mixture Used for Adsorption (wt %)						Purity of HMF from Methanol Desorption Effluent (wt %)	
Cycle #	IL	Unk	Glu	Fru	HMF	H_2O	#1-Peak Position	#2-Next to the Peak
5	57.79	2.13	0.11	0.45	2.98	36.53	100.2	97.9
6	56.34	2.16	0.00	0.44	2.91	38.15	98.5	98.7
7	58.79	1.53	0.11	0.45	2.95	36.16	98.2	92.1
8	62.59	1.71	0.09	0.69	3.18	31.74	99.9	92.9

column in the adsorption process. HMF breakthrough occurred about 40 min later than the IL and the selective HMF adsorption is clearly shown. However, the HMF breakthrough curve does not appear to be a steep S curve. We believe that a sharp adsorption front can be obtained by optimizing the flow conditions such as liquid flow velocity and bed design parameters such as aspect ratio. The desorption profiles in Figure 7b show that the residual IL and feed mixture was quickly washed out of the column by water, and their content in the effluent declined to zero in 20 min. The presence of small amounts of HMF in the water-flushing effluent was likely due to desorption of weakly bonded HMF. Upon switching to methanol flushing, the adsorbed HMF was rapidly desorbed. HMF content in the effluent reached a peak and then declined to zero. HMF content at the peak is 9.2%. Compared to 2.5% in the original feed solution, 3.7-fold enrichment of HMF is obtained.

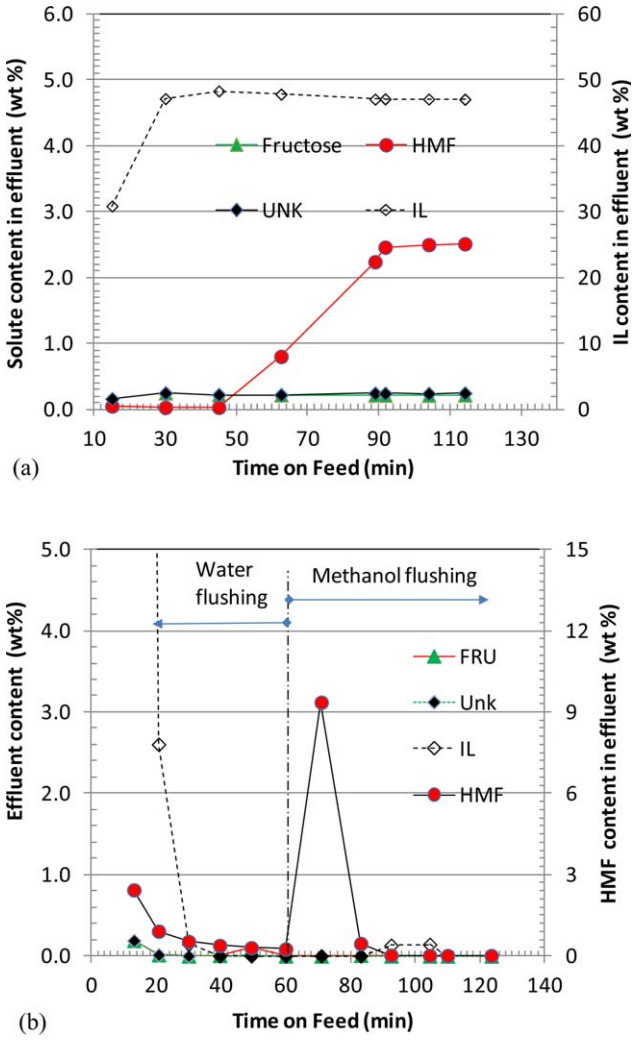

Figure 7. Adsorption and desorption profiles of the column packed with silicalite/OPZ particles (temperature: 50°C; adsorption feed: 47.2% IL, 0.0% glucose, 0.206% fructose, 0.055% formic acid, 2.50% HMF, and 0.218% unknown)

(a) Adsorption breakthrough profile (flow rate = 1.41 cm^3/min) and (b) regeneration profile (water flushing = 0.94 cm^3//min, methanol flushing = 0.80 cm^3/min). [Color figure can be viewed in the online issue, which is available at wileyonlinelibrary.com.]

By comparing Figure 8 to 7, we can see that the silicalite/silicalite particle provides better separation of HMF from the reaction mixture during adsorption and more efficient regeneration than the silicalite/OPZ particle. HMF adsorption breakthrough started at 92 min for the silicalite/silicalite particle (Figure 8a) and at 46 min for the silicalite/OPZ column (Figure 7a) at the same feed flow rate. After adsorption, the residual IL was more rapidly washed out of the column by water for the silicalite/silicalite (Figure 8b) than for the silicalite/OPZ adsorbent (Figure 7b). Only HMF was eluted from the silicalite/silicalite column during the subsequent methanol flushing, which enables recovery of 99% pure HMF. By contrast, there was still some IL coming out of the silicalite/OPZ column in the late state of the methanol flushing. HMF content in the first effluent sample during the methanol flushing of the silicalite/silicalite column was as high as 9.57%, whereas the adsorption feed contained only 1.46% HMF. 6.5-fold enrichment of HMF is shown. The adsorption/regeneration profiles illustrate excellent separation performances of the pure silicalite/silicalite adsorbent particle.

The results from three adsorption/regeneration cycles are summarized in Table 5 for the two particle-packed columns. These tests were conducted with the reacted IL mixtures under similar conditions. Low pressure drops were obtained with the particle bed as expected. The pressure drops for the IL solution to flow through the column during the adsorption were in the range of 0.6–1.4 bars. Typically, 1.0 cm^3/min of the adsorption feed flow rate was used. The variations in the pressure drop were mainly due to deposition of the IL and residual particulate on the flow distributor of the column rather than due to the adsorbent bed itself. The porous metal foam discs were placed on the top and bottom of the adsorbent column as a flow distributor. The pressure drop for the particle bed is reasonable for practical adsorption processes. The larger pressure drops observed with the silicalite/OPZ particle during first two cycles of water flushing were due to partial plugging of the distributor. The water-flushing rate was maintained constant around 1.0 cm^3/min for these cycles. 0.80 cm^3/min of the methanol-flushing rate was used for the HMF recovery. The pressure drops were very small for all the runs with methanol flushing, which were in the range from zero (could not be measured) to 0.27 bars. The variation was again due to the distributor. Methanol is an

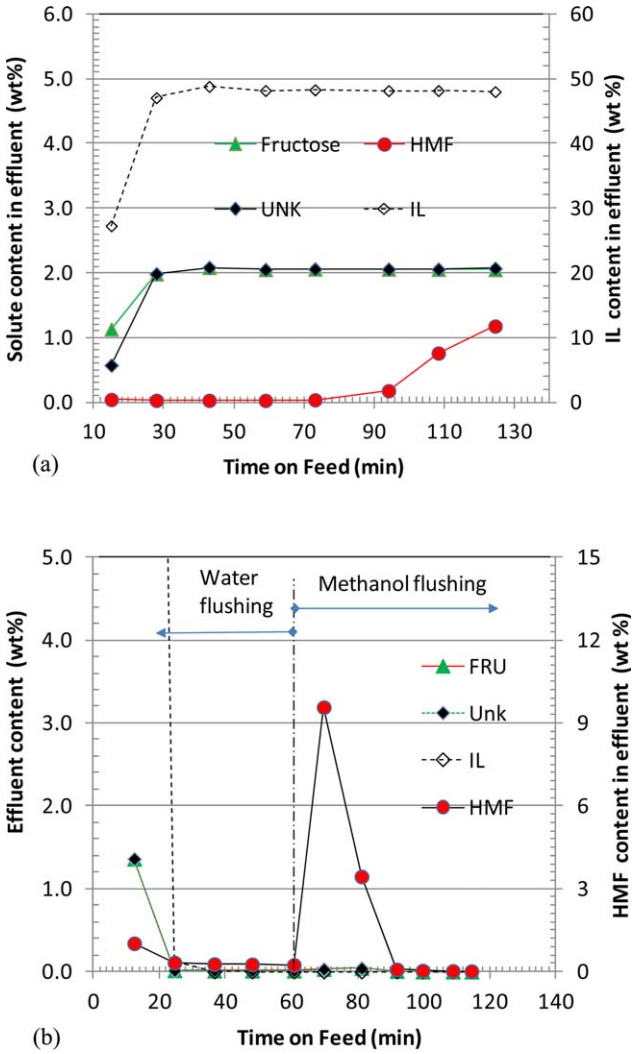

Figure 8. Adsorption and desorption profiles of the column packed with silicalite/silicalite particles (temperature: 50°C; feed mixture: 48.0% IL, 0.0% glucose, 0.205% fructose, 0.036% formic acid, 1.46% HMF, and 0.206% unknown)

(a) Adsorption breakthrough profile (flow rate = 1.02 cm^3/min) and (b) regeneration profile (water flushing = 1.0 cm^3/min, methanol flushing = 0.85 cm^3/min). [Color figure can be viewed in the online issue, which is available at wileyonlinelibrary.com.]

effective cleaning solvent for removal of the deposit on the distributor. For large-scale adsorbent beds, a flow distributor different from the metal foam used in the current laboratory tests will be needed.

The HMF desorption capacities listed in Table 5 were calculated based on the amount of HMF collected in the effluent during the water and methanol flushing, respectively. The HMF eluted with the water flushing is attributed to the residual feed solution and weakly adsorbed HMF on the exterior surface of a zeolite crystal, whereas the HMF released during the methanol flushing is considered due to desorption of HMF adsorbed inside the zeolite pore. First adsorption/regeneration cycle often did not reflect the working state of the adsorbent and column. The column typically reached a stable working state in the subsequent adsorption/regeneration cycles. For the silicalite/OPZ particle, HMF desorption capacities reached about 4% for the water flushing and 9% for the methanol flushing in the third adsorption/regeneration cycle. By contrast, HMF desorption capacities for the silicalite/silicalite column were about 2.5% for the water flushing and 12% for the methanol flushing. In other words, the silicalite/silicalite particle provided lower water desorption capacity but higher methanol desorption capacity than the silicalite/OPZ particle. This kind of performance is highly desirable for a practical adsorption process. The performance difference between these two adsorbents is explained by higher crystal purity and denser packing of the silicalite/silicalite particle as revealed by SEM analyses (Figures 2 and 3).

The material balances for Cycle #3 (Table 5) of the silicalite/silicalite particle bed showed 99% of the IL recovery and 96% recovery of HMF. Less than 100% recovery is attributed incidental loss during experiments.

Membrane-coated particle for separation of cellulose-derived IL reaction mixtures

Broad application of the present adsorbent to HMF separation from various reaction mixtures is illustrated by adsorption/regeneration tests with a feed solution different from those used above. The new feed solution was derived from water extraction of cellulose reaction in an [EMIM]Cl IL with addition of $CrCl_2$ and $CuCl_2$ catalysts.[16] The reacting mixture was quenched with deionized water and the resulting solution was filtered prior to adsorption tests. The IL and HMF content in the new feed mixture are 35.0 and 0.65%, respectively. The adsorption tests were performed on the column loaded with the silicalite/OPZ particle, and representative adsorption and regeneration profiles are plotted in Figure 9. The adsorbent fully captured the HMF in the feed, though HMF content was substantially less in this adsorption feed than in the previous runs. Due to the small HMF content in the feed, it took about 3 h for the HMF breakthrough to occur. Figure 9b shows that the residual IL solution after adsorption was washed out of the bed completely by the water. The adsorbed HMF was rapidly released upon introduction of methanol flushing. The HMF level in the initial methanol-flushing effluent was 6.32–5.35%, which is about 10-fold enrichment from the feed. The adsorption capacities with this feed solution are listed in Table 6. The HMF adsorption capacities from the methanol flushing were 7.11 and 7.67% for the two consecutive adsorption/regeneration runs. These capacity values are slightly lower than those obtained on the same column but with the previous IL reaction mixture (Table 5). This can be explained by the difference in HMF content between the two adsorption feeds used. The variation in the HMF capacity obtained from the water flushing was mostly caused by the state of the adsorbent bed at termination of individual adsorption runs. In the first run, the adsorption was stopped after complete HMF breakthrough, whereas the adsorption was stopped at the beginning of HMF breakthrough in the other run.

The testing results with the [EMIM]Cl IL mixture confirms that the present adsorbent can be used to separate HMF from other IL or solution mixtures due to its molecular specificity.

Conversion of unknown species in recovered IL

After HMF product is separated out of a reaction mixture, reuse of the recovered IL and conversion (or disposal) of the

Table 5. Testing Results of Engineered Particle-Packed Columns with Reaction Mixtures of Fructose + Fresh Ionic Liquid (Adsorption Feed Rate: 1.0 cm^3/min; Water-Flushing Rate: 1.0 cm^3/min; Methanol-Flushing Rate: 0.8 cm^3/min)

	Adsorption		Desorption ΔP (bar)		HMF Desorption Capacity	
Cycle #	HMF in Feed (%)	ΔP (bar)	Water Flushing	Methanol Flushing	Water (%)	Methanol (%)
Silicalite/OPZ particle						
1	2.45	0.75	16.2	0.07	2.43	5.59
2	2.49	1.16	17.1–34.2	0.07	4.68	8.63
3	2.50	0.96	0.55	0.00	3.98	9.00
Silicalite/silicalite particle						
1	2.52	0.89	0.68	0.00	7.07	20.9
2	1.44	0.96	0.48	0.00	2.93	11.8
3	1.46	0.96	0	0.00	2.45	11.9

remaining constituents in it (including the unknown and unconverted sugars) are critical issues for development of an economic HMF production process. It happens that the unconverted sugars and unknown species (Unk) elute together with the IL from the present adsorption column. As a result, these two issues can be addressed together.

The recovered IL was heated in the glass batch reactor at different temperatures without any addition of fresh fructose to assess reactivity of those remaining compounds. The recovered IL contained 1.97% unknown (Unk), 0.143% glucose, 0.45% fructose, and 0.88% HMF. The 0.45% fructose was from unconverted feed. The unknown and glucose were produced from original fructose reactions in the fresh IL. The presence of a significant amount of HMF was due to recycling of HMF-containing raffinate and water-flushing effluents. Figure 10 shows variations of the IL composition and temperature with time. As the temperature was increased from 26 to 80°C in 80 min, a slight increase in all the three species (unknown, HMF, and fructose) was observed. This is explained by slight concentration of the IL due to vaporization of residual water. As the temperature was further raised from 80 to 110°C in 23 min, the unknown species (Unk) decreased concomitantly with increase of the fructose and HMF. Such changes suggest disproportionation reaction of the unknown into HMF and fructose. With further increase of the temperature to 116°C in 80 min, the unknown (Unk) continued declining and HMF continued increasing, while fructose decreased. The decrease of fructose was attributed to conversion of fructose into HMF and unknown (Unk). It is interesting to note that glucose slightly decreased during 80 min heating from 110 to 116°C. Compared to its initial composition, heating the recovered IL can reduce the unknown (Unk) and glucose content while increasing HMF content. This important finding suggests that the unknown and glucose would not accumulate in recycled uses of the IL. Thus, it may not be necessary to separate the unknown out of the reaction mixture. The test below further validates this point.

Conversion of fresh fructose in recovered IL

The recycled IL was used for conversion of fresh fructose under a constant temperature. Figures 11a and b show variations of major compounds in the reaction mixture with time at reaction temperatures of 110 and 130°C, respectively. The IL used in the 110°C-run contained 1.21% unknown, 0.106% glucose, 0.66% fructose, and 1.35% HMF. To this IL, 9.8% of fresh fructose was added. At 110°C, the fructose content monotonically decreased while HMF content increased with time (Figure 11a). The unknown (Unk) increased with time initially, reached a peak and then decreased with time. This kind of production characteristic reflects two opposite reactions going on: formation of the unknown from fresh fructose, conversion of the unknown into HMF. The glucose content stayed at a low level.

Fructose conversion (X_F), HMF selectivity (S_{HMF}), and unknown selectivity (S_{Unk}) are calculated from the batch reactor testing results with the following equations

$$X_F = 1 - \frac{W_B \cdot \omega_F}{W_{0,IL} \cdot \omega_{0,F} + W_{0,F}} \quad (1)$$

$$S_{HMF} = \frac{n_{B,HMF} - n_{0,HMF}}{n_{0,F} - n_{B,F}} \quad (2)$$

$$S_{Unk} = \frac{n_{B,Unk} - n_{0,Unk}}{n_{0,F} - n_{B,F}} \quad (3)$$

In the above calculation, the presence of fructose, HMF, and unknown species in the original recycled IL is taken into account. The selectivity is calculated based on carbon numbers. In the calculation, we assumed the unknown species be the sugar molecule minus one H_2O molecule (MW = 162) and used fructose's HPLC response factor to determine the unknown content from HPLC peak areas. The conversion and selectivity values at different reaction times are tabulated in Table 7. Initially, the selectivity toward HMF was less than 1.0 because a fraction of fructose was converted into the unknown. At deep fructose conversion (95–98%), the HMF selectivity was more than 1.0 with little or no selectivity toward the unknown. The greater than 1.0 selectivity toward HMF was caused by conversion of the original unknown into HMF and/or inaccuracy in quantification of the unknown. In fact, the unknown are composed of several compounds and their molecular identities are unknown currently. Recognizing the uncertainty in the unknown quantification, we think it is reasonable to conclude that fresh fructose feed can be converted into HMF almost stochiometrically without any increase of the unknown and glucose in the IL from their starting level.

The IL solution used for the test at 130°C was recovered from a different adsorption separation run. It contained higher unknown (Unk), higher HMF, and lower fructose. 9.1% of fresh fructose was charged into this IL. By comparing Figure 11b to 11a, we can see that fructose in the IL was extremely reactive at 130°C and nearly complete conversion occurred within 10 min. Production of the unknown showed a peak initially and declined later, which is similar to the reaction at 110°C. However, HMF production reached a peak and then started gradual declining, as compared to a plateau reached at 110°C. The reaction selectivity at this temperature is compared to that at 110°C in Table 7. The HMF selectivity at 130°C is consistently less than 1.0. One

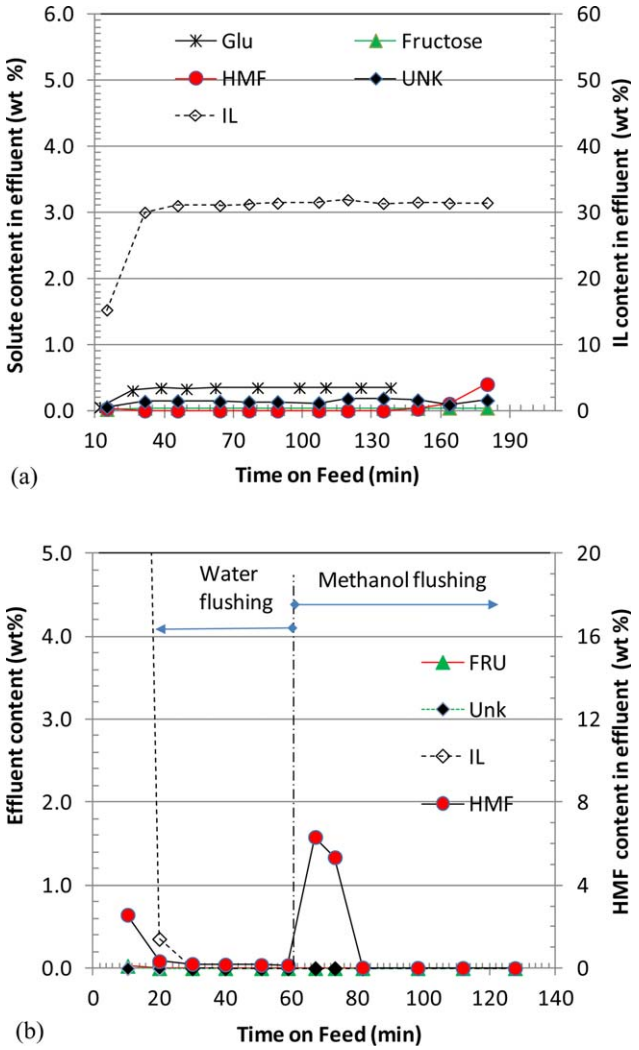

Figure 9. Adsorption and desorption profiles of the column packed with silicalite/OPZ particles (temperature: 50°C; water extract of cellulose +[EMIM]Cl reaction mixture: 30.9% IL, 0.095% glucose, 0.037% fructose, 0.064% formic acid, 0.678% HMF, and 0.0% unknown)

(a) Adsorption breakthrough profile (flow rate = 1.0 cm^3/min) and (b). regeneration profile (water flushing = 0.96 cm^3/min, methanol flushing = 0.78 cm^3/min). [Color figure can be viewed in the online issue, which is available at wileyonlinelibrary.com.]

probable cause for the lower HMF selectivity is side reactions and loss of HMF during reaction. HMF vaporization rate increases exponentially with temperature. HMF loss due to vaporization could become significant at 130°C.

Reaction equations

Based on our previous kinetics studies with fresh ILs[20] and present testing results with recovered ILs, we propose the following reaction equations involved in the conversion of fructose into HMF

$$\text{Fructose} \rightarrow \text{Intermediates (Unk)} + \text{H}_2\text{O} \quad \text{(fast)} \tag{4}$$

$$\text{Intermediates (Unk)} \rightarrow \text{HMF} + 2\text{H}_2\text{O} \quad \text{(slow)} \tag{5}$$

$$\text{Fructose} \rightarrow \text{HMF} + 3\text{H}_2\text{O} \quad \text{(moderate)} \tag{6}$$

$$\text{Fructose} + \text{HMF} \leftrightarrow \text{Intermediate (Unk)} \quad \text{(fast)} \tag{7}$$

$$\text{Fructose} \leftrightarrow \text{Glucose} \quad \text{(minor)} \tag{8}$$

$$\text{HMF} \rightarrow \text{Condensation or polymeric products (negligible)} \tag{9}$$

Formation of levulinic and formic acid was not detected in the present tosylate IL reaction system. The unknown species are likely reaction intermediates. They are stable under the present adsorption separation conditions (50°C in water and methanol). They are formed concomitantly with HMF when fructose feed is added into a fresh IL. Fortunately, these reaction intermediates in the same IL can be converted back into HMF and fructose by heating, after fraction of produced HMF is separated out. Thus, stoichiometric conversion of fresh fructose feed into HMF is possible by utilizing the recycled IL and conducting reaction under suitable conditions without increasing content of the unknown and sugars from its starting level in the recycled IL.

Process flow diagram for a practical HMF production process

A complete production process of HMF from fructose is conceived based on the research results obtained in this work. Figure 12 shows a simplified process flow diagram with major equipment, inputs and outputs identified. Ancillary equipment, such as heat exchangers, condensers, heaters, and pumps, is not included. The process flow is briefly described as follows. Fresh sugar feed is mixed with the recycled IL through an online mixer (M-1) such as a twin screw extruder, and the mixture is fed into the reactor (R-1). The reactor may be stirred mechanically and/or lifted using a purge gas stream. For example, a countercurrent flow reactor can be used. The reactor is preferably operated at temperatures above 100°C and nearly atmospheric pressure to avoid condensation of liquid water inside the reactor. The water vapor produced by the dehydration reaction is continuously stripped out of the reactor by the purge gas. The purge gas stream exited from the reactor is cooled down so that the entrained water vapor is condensed into liquid water. The condensed water is stored in a container (C-1), whereas the purge gas is recycled to the reactor. A fraction of the produced water can be used to flush the saturated adsorbent bed (A-2), whereas the rest is discharged as a waste water stream. The reacted IL mixture is discharged at the bottom of the reactor. Upon existing from the reactor, the reacted IL stream is mixed with a cold water stream. An online static mixer (M-2) may be used. Addition of the cold water is to quench the reaction and adjust the viscosity and temperature of the fluid for the adsorption process. The potential solid particulate matter in the mixed stream is removed through a filter (F-1). The filtered stream is fed into the adsorption column (A-1). A simple two-bed adsorption system is proposed in this process so that adsorption and regeneration can be alternated between the two beds. HMF in the reaction mixture is captured on the adsorbent bed. The raffinate stream, which consists of unconverted sugars, unknown intermediates, IL, and water, is sent to a dewatering unit (D-1). The removed water is reused to quench the reactor effluent, whereas the IL substantially free of water is recycled for the catalytic reaction.

The saturated adsorbent bed (A-2) is first purged with an inert gas stream to remove the free volume of the fluid left

Table 6. Testing Results of Silicalite/OPZ Particle-Packed Column with Water Extract of Cellulose+[EMIM]Cl Ionic Liquid Mixture

	Adsorption		Desorption ΔP (bar)		HMF Desorption Capacity	
Cycle #	HMF in Feed (%)	ΔP (bar)	Water Flushing	Methanol Flushing	Water (%)	Methanol (%)
1	0.678	0.21–1.1	1.03	0	2.89	7.11
2[a]	0.650	0.21–1.1	1.03	0	0.06	7.67

[a]HMF breakthrough did not occur during adsorption

from the adsorption process. Then, the saturated bed is washed with water. The liquid effluent during the gas purge and water flushing is saved and stored in a container (C-2), which can be sent back to the adsorption bed because its composition would be similar to the original adsorption feed. After all the residual IL and adsorption feed are washed out of the bed, the washing fluid is switched from water to methanol. The HMF adsorbed on the zeolite crystal is desorbed by methanol. Majority of the column effluent during the methanol flushing is stored in a container (C-3), whereas the tail portion of the methanol flushing is stored in the container C-4 in case there might be some byproducts other than HMF retained in the adsorbent. The methanol effluent stored in C-3 contains only HMF and is sent to a demethanol unit (D-2) to produce a pure HMF product. The effluent stored in C-4 is sent to a demethanol unit (D-3) to produce a possible byproduct if there is any.

In the process flow diagram of Figure 12, fructose is the main feed stream, HMF is the main product stream, and waste water is the main possible waste stream. Other feed streams (IL, water, methanol, and purge gas) are mainly used for start-up and become supplementary in normal plant operation. The IL and methanol will be fully recycled. The supplementary inputs are only to compensate the incidental process loss. Conversion of each sugar molecule into HMF produces three molecules of water. Thus, no fresh water is needed in normal operation. Discharge of some waste water may be necessary to avoid water accumulation in the recycle loop. It is noted that methanol used in this work is one example of solvent for HMF desorption, and other solvents may work as well as methanol.

The reactor and adsorbent beds are the critical, new equipment for the proposed process. Operation conditions and sizes of these two units at fructose processing capacity of 200,000 ton/year are estimated based on the experimental

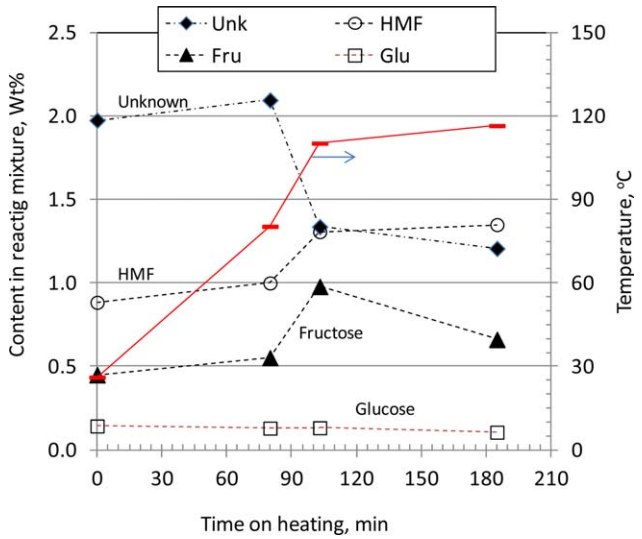

Figure 10. Impact of heating on conversion of reaction intermediates (Unk) in a recovered IL without addition of any new fructose feed (IL composition: 1.97% Unk, 0.143% glucose, 0.45% fructose, and 0.883% HMF).

[Color figure can be viewed in the online issue, which is available at wileyonlinelibrary.com.]

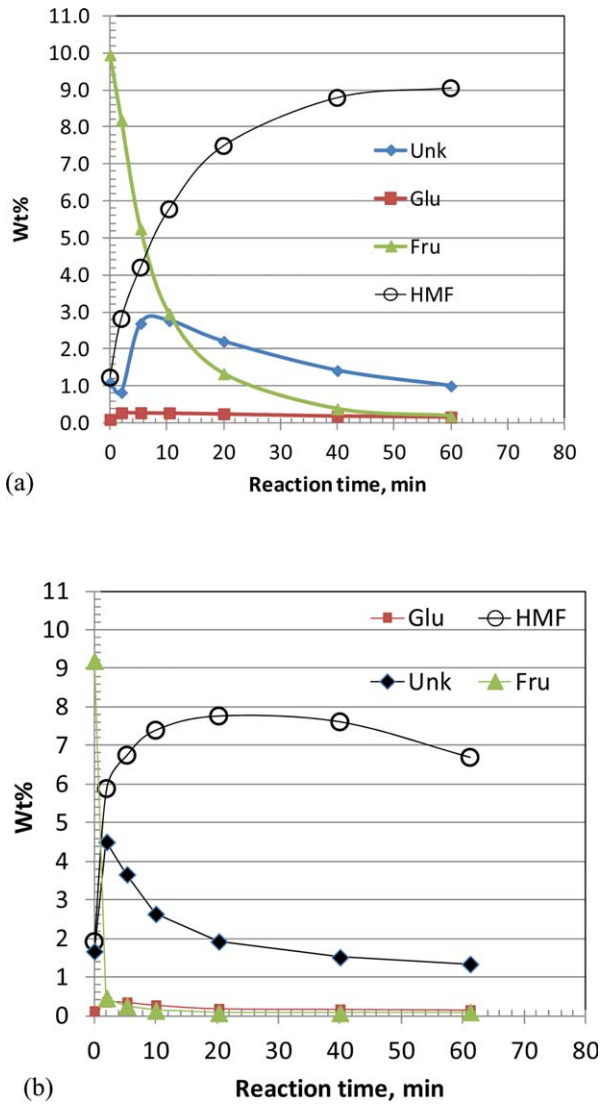

Figure 11. Conversion of fresh fructose in the recovered IL

(a) 110°C (recovered IL composition: 1.21% Unk, 0.106% glucose, 0.661% fructose, and 1.35% HMF) and (b) reaction temperature of 130°C (recovered IL composition: 1.84% Unk, 0.145% glucose, 0.102% fructose, and 2.11% HMF). [Color figure can be viewed in the online issue, which is available at wileyonlinelibrary.com.]

Table 7. Conversion of Fresh Fructose with Recovered Ionic Liquid in a Batch Reactor

Reaction Run at 110°C[a]				Reaction Run at 130°C[b]			
		Selectivity (mol/mol)				Selectivity (mol/mol)	
Time (min)	Fructose Conversion	To HMF	To Unk	Time (min)	Fructose Conversion	To HMF	To Unk
2	0.214	1.023	−0.132	2	0.950	0.648	0.360
5.3	0.496	0.823	0.344	5.3	0.972	0.772	0.248
10	0.717	0.871	0.250	10	0.985	0.864	0.119
20	0.872	0.985	0.136	20	0.992	0.916	0.031
40	0.964	1.077	0.036	40	0.992	0.892	−0.019
60	0.982	1.093	−0.010	61	0.989	0.750	−0.040

[a]39.35 g of the recycled ionic liquid used: 1.13% unknown, 0.117% glucose, 1.15% fructose, and 1.494% HMF. 3.91 g of fresh fructose was added when the ionic liquid was stabilized at 110°C.
[b]14.63 g of the recycled ionic liquid used: 1.84% unknown, 0.145% glucose, 0.102% fructose, and 2.11% HMF. 1.461 g of fresh fructose was added when the ionic liquid was stabilized at 130°C.

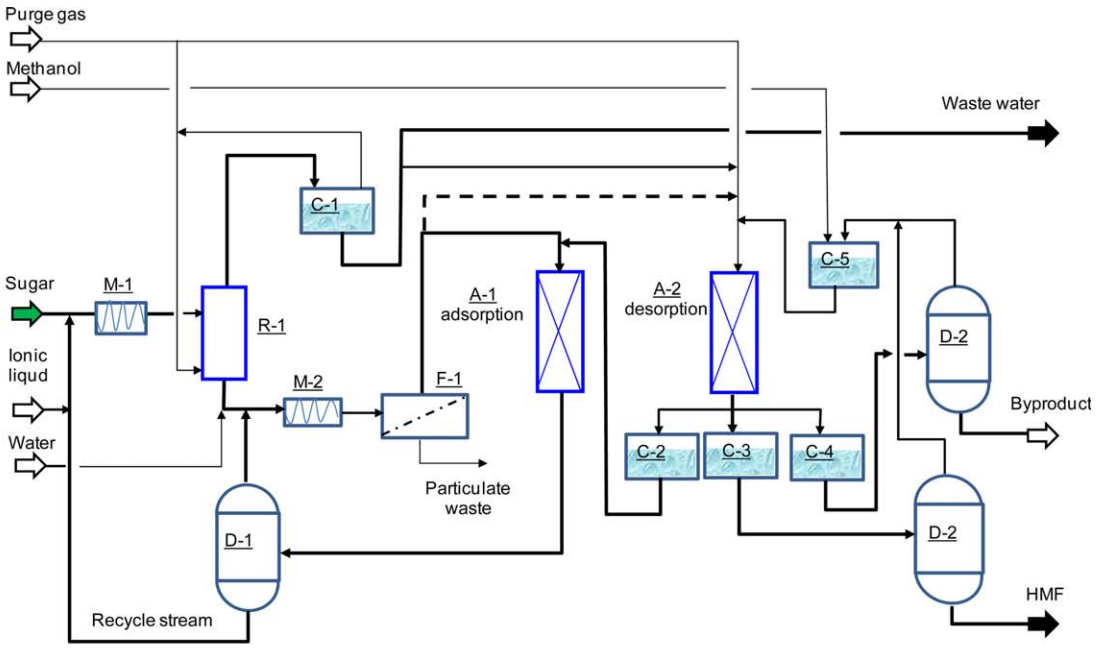

A-1	Adsorbent bed under adsorption operation	D-1	Removal of water from the recycled stream
A-2	Adsorbent bed under regeneration operation	D-2	Removal of methanol from HMF/methanol solution
C-1	Separation of purge gas from condensed water product	D-3	Removal of methanol from Heavier/methanol solution
C-2	Storage of gas purge and water-flushing effluents	F-1	Removal of particulate from the mixed solution
C-3	Storage of methanol-flushing effluent	M-1	Online mixer of ionic liquid and sugar
C-4	Storage of residual effluent from methanol flushing	M-2	Online mixer of reacted ionic liquid mixture and water
C-5	Storage of methanol - regeneration solvent	R-1	Reactor with continuous stripping of water vapor product

Figure 12. A complete IL process for conversion of fructose into HMF.

[Color figure can be viewed in the online issue, which is available at wileyonlinelibrary.com.]

Table 8. Projected Sizes of Reactor and Adsorbent Beds for an Industrial Process (Fructose Processing Capacity: 200,000 T/year; HMF Output: 140,000 T/year)

Reactor		Adsorbent Bed		Recycled Ionic Liquid	
Temperature (°C)	110	Temperature (°C)	50	Composition	%
Pressure (bar)	1.20	Pressure drop (bar)	2	Intermediates (Unk)	1.21
Residence time (min)	40	Adsorption time (min)	40	Glucose	0.11
Fructose feed/IL (w/w)	1:9	HMF recovery (%)	85.2	Fructose	0.66
One-pass fructose conversion (%)	94.4	Packing density (kg/L)	0.54	FA	0.00
HMF selectivity (mol %)	100	HMF capacity (%)	12.0	LA	0.00
Void fraction	0.40	Void fraction	0.35	HMF	1.35
Reactor volume (m^3)	264	Volume of each bed (m^3)	180	IL	96.68
Ionic liquid charge (ton)	232	Total adsorbent (ton)	194	Total	100

results achieved in this work. Important process conditions and unit design parameters are summarized in Table 8. Stoichiometric conversion of fructose into HMF is assumed. A recycled IL stream of similar compositions to what was tested in the batch reactor run shown in Figure 11a is used to establish steady-state process flow streams. The reactor is fed with fructose/IL ratio of 1/9 by weight and assumed operating at one-pass fructose conversion of 94.4%, which corresponds to complete conversion of fresh feed. The estimated reactor volume is about 264 m^3 at a liquid residence time of 40 min and the IL inventory is about 232 ton. The individual adsorbent bed volume is estimated to be about 180 m^3 at 40-min adsorption/regeneration cycle time with an adsorbent of 12% HMF adsorption working capacity and 0.54 kg/L packing density. The total adsorbent weight for the two beds is about 194 ton. These numbers are in line with typical petrochemical processes.

It is noted that the operation conditions listed in the Table 8 are only as an example and do not represent the optimum yet. The reactor and adsorbent bed sizes can be reduced with further process development and optimization. For example, the reactor size and IL inventory will be decreased if the higher fructose loading (20%) in the IL and/or short residence time (10–20min) are used. The adsorbent bed size and adsorbent inventory can be reduced if the adsorption packing density is increased and/or the regeneration cycle time is shortened.

The proposed HMF production process from fructose is much simpler than the PX manufacturing process from petroleum oil.[7] The proposed reactor and adsorbent bed are all operated under very moderate conditions (<150°C, atmospheric or low pressures <10 bar), as compared to the catalytic reactors (>300°C, >20 bar, large volume of H_2) often used in current aromatics conversion processes. Isolation of pure HMF product from the reaction mixture with the adsorption technology shown in this work is also simpler than separation processes (crystallization or simulated moving bed) used to obtain pure PX from C8 aromatics. Thus, the proposed HMF production process has large potential to obtain significant energy savings and capital cost reduction, compared to petroleum-derived chemical feedstock.

If HMF product value is assumed to be the same as current PX product on the basis of equivalent mole of aromatic ring, the HMF product value would be $1.21/kg at PX market price of $1.44/kg. At assumption of fructose cost of $0.46/kg, there can be significant gross margin for HMF production.

Remaining issues and future work

Presence of a significant amount of reaction intermediates is reported first time by this work. For production of commodity chemicals, the product selectivity or carbon atomic efficiency is very important. Although the present work suggests that the accumulation of these unknown intermediates in the recycled IL might be avoided by making complete conversion of fresh fructose feed into HMF under suitable reaction conditions, the future work is recommended to determine molecular structures of these unknown species for the purposes of both fundamental chemistry understandings and practical process development.

As the reaction mixture and adsorption feed volumes involved in the present studies were in tens of grams and still small, mass balances could be drastically affected by those uncontrollable variations, such as uncertainty of the state of the column and incidental loss during sample handling. The long-term stability of the IL is not known yet. Thus, a pilot plant needs to be built and run in long-time continuous operation for the purposes of (1) producing a significant amount of HMF for product development, (2) conducting accurate material balances, (3) demonstrating long-term stability of the IL, and (4) determining the IL loss rate. Detailed process simulation should be performed for process economics analysis.

Summary

Two critical technology problems for development of a practical HMF production process from sugars are addressed by this work. The first problem is about separation of pure HMF product from reaction mixtures in an economic and energy-efficient way. The silicalite-based adsorbent materials provide high-HMF adsorption capacity (12%) and selective HMF adsorption over other molecules. Isolation of 99% pure HMF from actual IL reaction mixtures and recovery of the IL, unconverted sugar, and reaction intermediate are shown with an adsorbent column operated at 50°C. Scale-up possibility of the adsorption process is shown by preparing novel membrane-coated adsorbent particles that allow the adsorption process to be conducted at moderate pressure drops and provide better separation performances than the powder material. The second problem is about recycling and reuse of the IL. The reaction tests confirmed that the recycled IL is active and selective for conversion of fresh fructose feed into HMF. Accumulation of unconverted sugars and reaction intermediates in the recycled IL can be avoided by conducting the reaction under suitable conditions (temperature, time). As a result, stoichiometric conversion of fructose into HMF is possible. This unique catalytic attribute of the IL enables efficient utilization of fructose, which is very important for a practical process.

A simplified process flow diagram for industrial production is proposed based on the present innovations for further development, pilot plant demonstration, and process

engineering and economics analysis. The HMF production process form sugars can be much simpler than the current PX manufacturing process from petroleum oil. At equivalent value to PX on molar basis, there could be a large gross margin to manufacture HMF from fructose or sugars.

The adsorbent and adsorption technologies presented in this work can be used for separation of HMF or linear hydrocarbon-type products from other reaction mixtures made of different ILs and/or water solutions.

Acknowledgments

This contribution was identified by Professor Suojiang Zhang (Institute of Process Engineering, Chinese Academy of Sciences) as a "Best Presentation" in the session "International Forum on Energy Sustainability" of the 2012 AIChE Annual Meeting in Pittsburgh, PA. The authors would like to thank their colleagues, Dr. Tony Rao for adsorbent preparation, Dr. Abhijeet Karkamkar for conducting the TGA tests, and Mrs. Shari Li for BET surface area measurements. They also would like to thank Dr. John Holladay at PNNL, and Timothy Brandvold and Sharry Lynch at UOP for starting this project. This project was funded by USDA under Grant Agreement # 68-3A75-7-613.

Notation

$n_{0,F}$ = moles of total fructose present in the reactor at the beginning of reaction
$n_{B,F}$ = moles of fructose present in the reacting batch
$n_{B,HMF}$ = moles of HMF present in the reacting batch
$n_{0,HMF}$ = moles of HMF present in the recycled IL prior to reaction
$n_{B,Unk}$ = moles of unknown species present in the reacting batch
S_{HMF} = HMF selectivity
S_{Unk} = unknown selectivity
W_B = total weight of reacting batch
$W_{0,IL}$ = initial weight of recycled IL
$W_{0,F}$ = weight of fresh fructose added into reactor at the beginning of reaction
X_F = fructose conversion
ω_F = weight fraction of fructose in the reacting batch
$\omega_{0,F}$ = weight fraction of fructose in the recycled IL

Literature Cited

1. Sims B. *Coca-Cola Partners with Three Biotech Firms to Develop Bio-PET*. *Biorefining Magazine*, December 16, 2011. BBI International; http://brmagazine.eclipticcms.com/Issue.aspx.
2. Voegele E. Global Market for Bioplastics Expected to Grow Significantly. *Biorefining Magazine*, January 5, 2012. BBI International; http://brmagazine.eclipticcms.com/Issue.aspx.
3. Global Industry Analysts Inc. Polyester: a global strategic business report, Report Code MCP-2124. Global Industry Analysts Inc., 2012. http://www.marketresearch.com/corporate/aboutus/.
4. Peters MW, Taylor JD, Jenni M, Manzer LE, Henton DE. US Patent 2011/0087000 A1, October 6, 2010.
5. Kunz M. Hydroxymethylfurfural, a possible basic chemical for industry intermediates. In: Fuchs A, editor. Inulin and Inulin-Containing Crops. Elsevier Science Publishers B.VL: Amsterdam, The Netherlands., 1993. pp. 149–160.
6. Werpy T, Petersen G. Top value added chemicals from biomass—technical report no. DOE/GO-102004-1992. Golden, CO: National Renewable Energy Lab, 2004.
7. Cannella WJ. Kirk-Othmer Encyclopedia of Chemical Technology. Xylenes and Ethylbenzene. John Wiley & Sons, Inc. doi:10.1002/0471238961. October 19, 2007.
8. Rosatella AA, Simesonov SP, Frade RFM, Afonso CAM. 5-Hydroxymethylfurfural (HMF) as a building block platform: biological properties, synthesis and synthetic applications. *Green Chem.* 2011; 13:754–793.
9. van Putten R, van der Waal JC, Jong ED, Rasrendra CB, Heeres HJ, de Vries JG. Hydroxymethylfurfural, a versatile platform chemical made from renewable resources. *Chem Rev*. In press.
10. James OO, Maity S, Usman LA, Ajanaku KO, Ajani OO, Siyanbola TO, Sahu S, Chaubey R. Towards the conversion of carbonhydrate biomass feedstocks to biofuels via hydroxylemethylfurfural. *Energy Environ Sci.* 2010;3:1833–1850.
11. Tong X, Ma Y, Li Y. Biomass into chemicals: conversion of sugars to furan derivatives by catalytic processes. *Appl Catal A*. 2010;385: 1–13.
12. Roman-Leshkov Y, Chheda JN, Dumesic JA. Phase modifiers promote efficient production of hydroxymethylfurfural from fructose. *Science*. 2006;312:1933–1937.
13. Torres AI, Daoutidis P, Tsapatsis M. Contineous production of 5-hydroxylemethylfurfural from fructose: a design case study. *Energy Environ Sci.* 2010;3:1560–1572.
14. Kazi FK, Patel AD, Serrano-Ruiz JC, Dumesic JA, Anex RP. Techoeconomic analysis of dimethylfuran (DMF) and hydrooxymethylfurfural (HMF) production from pure fructose in catalytic processes. *Chem Eng J*. 2011;169:329–338.
15. Zhao H, Holladay JE, Brown H, Zhang ZC. Metal chlorides in ionic liquid solvents convert sugars to 5-hydroxymethylfurfural. *Science*. 2007;316:1597–1600.
16. Su Y, Brown HM, Huang X, Zhou X, Amonette JE, Zhang ZC. Single-step conversion of cellulose to 5-hydrooxymethylfurfural, a versatile platform chemical. *Appl Catal A*. 2009;361:117–122.
17. Xie H, Zhao ZK. Selective breakdown of (ligno) cellulose in ionic liquids. In: Kokorin A, editor. Ionic Liquids: Applications and Perspective. InTech, Chapter 4, pp 61–80. February 21, 2011.
18. Stark A. Ionic liquids in the biorefinery: a critical assessment of their potential. *Energy Environ Sci.* 2011;4:19–32.
19. Tadesse H, Luque R. Advances on biomass pretreatment using ionic liquids: An overview. *Energy Environ Sci.* 2011;4:3913–3929.
20. Liu W, Holladay J. Catalytic conversion of sugar into hydroxymethylfurfural in ionic liquids. *Catal Today*. 2013;200:106–116.
21. Geier DF, Lenn Soper JG. Method for purifying hydroxymethylfurfural using non-functional polymeric resins. US Patent 7897794, June 18, 2008.
22. Liu W, Holladay J, Zheng F, Brown HM, Cooper AR. Adsorption separation processes for ionic liquid catalytic processes. US Patent 8236973, April 8, 2010.
23. Liu W, Rao Y, Karkamkar A, Liu J, Wang L. A Bubbling Reactor Technology for Rapid Synthesis of Uniform, Small MFI-type Zeolite Crystals. *Ind Eng Chem Res*. 2011;50:7241–7250.
24. Liu W, Zhang J, Canfield N, Saraf L. Preparation of Robust, Thin Zeolite Membrane Sheet for Molecular Separation. *Ind Eng Chem Res*. 2011;50(20):11677–11689.
25. Cytec Product document, CYPHOS-IL 106 Phosphonium Ionic Liquid. Cytec Product document. http://www.cytec.com.
26. Perry RH, Green DW. Perry's Chemical Engineers' Handbook. McGraw-Hill, 2007. 7th edition, online version.
27. Ventura SPM, Pauly J, Daridon JL, Lopes da Silva JA, Marrucho IM, Dias AMA, High pressure solubility data of carbon dioxide in (tri-iso-butyl(methyl)phosphonium tosylate + water) systems. *J Chem Thermodyn.* 2008;40 (8):1187–1192.

Manuscript received May 15, 2013, and revision received Aug. 30, 2013.